Extracting high precision information from CCD images

T.A. Clarke BSc PhD MInstPhys CPhys**, and Dr. X. Wang.** BSc MSc PhD Centre for Digital Image Measurement and Analysis, School of Engineering, City University, Northampton Square, LONDON. EC1V 0HB, UK

SYNOPSIS   In this paper several methods for utilising the full capabilities of CCD sensors are given. These methods are well known in the photogrammetric community but perhaps are less well known in other disciplines. This paper seeks to disseminate these techniques more widely and to provide a reference source for those who wish to use them.

1. INTRODUCTION

The CCD sensor has been widely used to measure heat transfer and fluid flow. The advantages are continuous and rapid capture of images which enable particles to be tracked and velocity fields to be measured. This paper discusses how this information can be extracted with the maximum fidelity starting with a model for the camera lens, progressing through image processing effects to consider correspondence issues before discussing the production of 3-D information from 2-D images, finally some practical issues are considered.

2. IMAGE CAPTURE

A standard model for lens distortion has evolved over many years in photogrammetry which has successfully been applied to lenses with a focal length from a few mm to a few hundred mm. If applied correctly subpixel precision of between 1/10 - 1/80th of a pixel is possible. Without this correction displacements of several pixels at the edge of the image format will be common. The primary source of lens error is due to symmetric distortion (barrel or pin cushion distortion). The secondary source of error (typically about 1/7 of symmetric lens distortion) is called decentring distortion. To define both it is necessary to estimate the focal length of the lens, the position of the image centre and the principal point (nominally the centre of radial lens distortion). The important features of this model are now given. The principal distance c is the

perpendicular distance from the perspective centre of the lens system to the image plane. At infinity focus, it is equal to the focal length c_0

$$c = c_0 + \Delta c \tag{1}$$

where Δc denotes the difference (offset). The principal point (x_P, y_p) is defined as that point on the image plane which is at the base of the perpendicular from the 'centre of the lens' or more correctly, from the rear nodal point.

$$x_p = x_0 + \Delta x_p, \quad y_p = y_0 + \Delta y_p \tag{2}$$

where (x_0, y_0), refers to the nominated centre of the sensor and $(\Delta x_P, \Delta y_p)$ are called the *principal point offsets*. Radial distortion is a symmetric effect and can normally be modelled by a polynomial series of odd powered terms, i.e.,

$$\Delta r = k_1 r^3 + k_2 r^5 + k_3 r^7 + \Lambda \qquad \text{where } r = ((x - x_p)^2 + (y - y_p)^2)^{\frac{1}{2}} \tag{3}$$

Δr is the radial displacement of an image point, k_1, k_2, and k_3 are the coefficients of the radial distortion corresponding, x and y are the co-ordinates of an image point. The displacement of the image point caused by the radial distortion is expressed as

$$\Delta x_r = (x - x_p)\frac{\Delta r}{r}, \quad \Delta y_r = (y - y_p)\frac{\Delta r}{r} \tag{4}$$

Δx_r and Δy_r are the corrections on x and y due to the radial distortion (Fig. 1). Typical C mount lenses can exhibit distortion at the edges of the image of up to 300 μm for a 6.5 mm lens and 30 μm for a 25 mm lens.

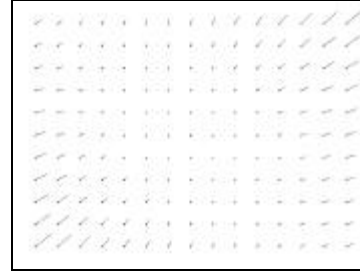**Figure 1. Radial lens distortion vectors**

Figure 2. Decentring lens distortion vectors

Decentring distortion is caused by misalignments of the lens elements and is described by two polynomials, one for the displacement in x direction and the other for the displacement in y direction (equ. 5) where p_1 and p_2 are two coefficients which are lens dependent, the other notations are the same as used in the radial distortion (Fig. 2).

$$\Delta x_d = p_1(r^2 + 2(x - x_p)^2) + 2p_2(x - x_p)(y - y_p), \quad \Delta y_d = p_2(r^2 + 2(y - y_p)^2) + 2p_1(x - x_p)(y - y_p) \tag{5}$$

Calibration of lenses in practical situations can be relatively simple, but it is not always possible to estimate all of the parameters by one method. The best methods will make use of redundant measurements and least squares to obtain statistics concerning the estimation process. It is worth noting that a first order correction can be applied relatively easily by approximating the

principal point offset with the sensor centre and using the first term only of the radial lens distortion (equ 3). It should be noted that the principal point offset can be up to 10% of the sensor size. The focal length can be estimated by placing two objects at a known distance apart at a distance from the camera which is long in comparison with the focal length of the lens (say 5-10 metres). An approximate measurement of the distance between the camera lens and the object together with the sensor pixel size and the standard lens magnification equation will yield a reasonable estimate of the focal length. Alternatively calibration may be achieved using 3-D methods which are described later. The principal point offset is not easy to obtain directly, laboratory methods (Shortis et al, 1995) are straight forwards while least squares estimation methods require sophisticated software and target test fields. To obtain the radial and decentring components, perhaps the most simple method uses the fact that straight lines in the object space should be straight lines in the image unless lens distortion is present. The parameters for lens distortion based upon the discrepancies between the model and the observed data. Straight lines may be constructed of retro-reflective tape, or stretched white lines. Finally it should be noted that all means of storage of data can introduce some error either in the initial A-D conversion or in the storage of information on video tape (Höflinger & Beyer, 1993) or disk using JPEG/MPEG compression techniques. Tape storage can introduce timing errors and changes of scale, while JPEG/MPEG is a lossy method and some loss of precision should be expected (Chen, et at. 1996).

3. IMAGE PROCESSING

There are a large number of error sources that are accumulated after the image of a target is formed on the sensor surface and digitisation. It should be noted that if there were no noise involved in the image sampling process (and a perfect lens were used) then it would be possible to locate the position of a target image perfectly even given discrete sampling positions. In practice every source of image acquisition error contributes to a degradation of measurement accuracy. Some of these sources of error are briefly explained.

(i) Poisson noise is an unavoidable source of noise in images which is the statistical fluctuation of light $\Delta N = \sqrt{N}$. This noise is more significant with small numbers of photons.

(ii) Charge transfer efficiency refers to the loss of charge as the charge accumulated at each photo site is moved to the readout stage. The efficiency is related to the number of times the charge is moved and becomes significant for large sensor arrays.

(iii) Signal to electronic noise ratio. Dark Current is reduced by about a half for every 8 degrees Celsius reduction in temperature so cameras with cooling will provide less noise. It is sometimes desirable to capture high speed events and some cameras are able to capture up to 1000 frames per second with a 12 bit converter. Faster conversion will lower dark current but increase readout noise, slow readout is necessary if noise levels are to be achieved.

(iv) Dynamic range is defined by the ratio of the charge capable of storage relative to the electronic noise. Currently the dynamic noise of a typical CCD sensor may be 1:few thousand but a typical scene may be 1:100,000. Seitz (1995) predicts that noise will be decreased and research results will become a reality and that a 60 dB improvement to 80 dB is within sight but 120 dB may ultimately be possible.

(v) Quantization. The analogue image information has to be measured to be of any use to a digital computer. In the process information is lost because an integer number is used to represent what is a continuously variable quantity. The quantization process can be shown (Clarke et al., 1993) to introduce significant errors into the target location process.

(vi) Some modern sensor exhibit considerable smearing of the image when nearing saturation due to blooming. If high intensity targets are used then it can be necessary to reduce the aperture to avoid the worst of this effect which will bias target location measurements.

(vii) Image sensor physical characteristics. Although not strictly an error source, the size of the pixels and the number of them has an effect on the overall positional accuracy. For many years the typical size of an image was 752x582 for the CCIR standard but now Philips 1K x 1K sensor can be butted to construct a 9k x 7k sensor, for example. The topology of the sensor may also be of some concern for large sensor. Small format sensors are only a few mm across but with larger sensors flatness variations can be a problem especially with short focal length lenses.

There are three basic methods for target image location: moments, least squares matching, and cross-correlation. Each method is capable of high accuracy target location under a variety of situations.

(i) The method of moments. There are four methods that could be chosen depending on the accuracy or speed required. **Average of perimeter**. This simple method averages the co-ordinates of the perimeter of the target image chosen with reference to a pre-selected threshold. **Binary centroid**. In this case all pixels over the threshold are equally weighted. **Grey-scale centroid**. With the grey-scale centroid the intensity values are used. **Squared centroid** method. In this case the intensity values are squared. For the first two methods the standard deviation for a small target is likely to be around 1/5 - 1/10 of a pixel getting better for a larger target. The final two methods are able to produce standard deviations of around 1/20 - 1/80 of a pixel. Targets are optimally around 7 pixels in diameter and care must be taken to achieve a high signal to noise ration and appropriate threshold values or biases in location can occur (Shortis, et al, 1994).

(ii) The method of least squares. There are three variants to this method: (a) functional model based fitting (Shortis, et al, 1994); (b) patch matching using a fixed template; and (c) patch matching using patches obtained from the imagery. In each case the objective is the same, the minimisation of the difference between the model or the patch and the section of the image which is deemed to have a target. In method a the model may be an ellipse or a Gaussian distribution. Least squared patch matching (Mitchell & Pilgrim, 1987, Ackermann, 1984, Gruen, & Baltsavias, 1987; Rosenholm, 1987; Hahn, 1993; & Mikhail, et al. 1984; Atkinson, 1996) involves producing an observation equation for each pixel in the patch to be matched which compares its intensity with the section of the image to which it is being matched.

(iii) Cross-correlation (Mitchell & Pilgrim, 1987; Ackermann, 1984). The cross-correlation method is probably familiar to many in this field and is particularly well suited to high particle densities so will not be discussed further.

With all subpixel location methods care must be taken to ensure that the quality of results is not compromised by other factors. For instance, it has been found that with a certain frame-grabber/camera combination a shift in location of reported pixel positions by as much as 4 pixels can occur during the warm-up period (Robson, et al. 1993). Hence, it is good practise to ensure that computer, frame-grabber, and camera are up to temperature before starting work. Other effects such as DC offset and line-jitter can also cause problems (Clarke, 1995; Beyer, 1990).

4. TARGET CORRESPONDENCES

This conventional situation for stereo is illustrated in figure 1. In this case correspondence can be computed with ease because first the epipolar lines in the first image line up with those in second image, and second, the images are usually obtained with only a small base length *b* so that they are radiometrically and geometrically similar except at positions where sharp discontinuities exist in the objects space. Hence, searching for correspondences only has to be performed for any feature or target in image 1 by searching along the corresponding line in image 2. A wealth of material has been produced to enable high reliability matching by using constraints to check for correct matching. Haralick and Shapiro (1993) discussed the use of epipolar geometry in image matching. They comment that "The epipolar line constraint is the strongest constraint in image matching and should be used as soon as available". Dhond and Aggarwal (1989) provided a comprehensive review of stereo research. It is often not possible to achieve the normal case of stereo pairs and it may also be undesirable because of the disadvantage of the configuration with respect to object coverage.
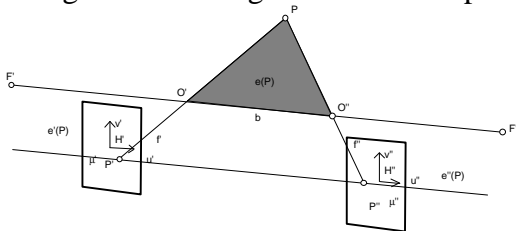

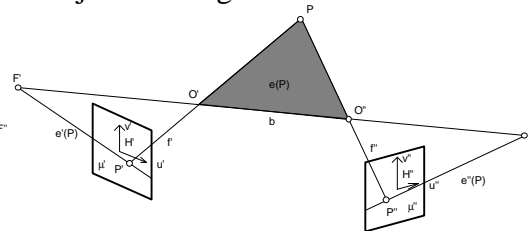**Figure 3. Normal case stereo pairs**   **Figure 4. Convergent views**

A conceptually simple approach to solving the correspondence problem with convergent geometry is to project the epipolar lines from features in image 1 into image 2. A search is required along the epipolar line to find homologous points. The disadvantage of this approach is the search must now be performed in two dimensions instead of one for each candidate. As a result it is common for images to be rectified to obtain conventional stereo pairs with the attendant benefits in terms of searching and ease of computation. If the interior and exterior parameters of the cameras are known then it is possible to rectify the images to provide images or target co-ordinates which have the same benefits as the normal case stereo pairs. Rectification can be achieved using either parametric methods or via collinearity equations, or non-parametric methods where a number of points on image 1 are used to compute the transformation necessary for image 2 (Marten, 1994). Another method adopted by Sabel, et al, (1993) is the comparison of slopes between images. Correspondences can also be computed by looking at the intersection between rays from features in each view and finding those that are the closest (Chen et al, 1993; Chen et al 1994). In fact this method is completely analogous to the epipolar line method. Back projection can be used as a means of propagating

correspondences from a pair of corresponding cameras onto a third or fourth using an estimate of the 3-D location of a target or feature to project the position of this point onto other images.

5. ESTIMATING 3-D FROM 2-D IMAGES

In photogrammetry multiple CCD cameras are used to capture images of targets viewed from a variety of angles. A set of so called *collinearity equations* can be derived to establish the relationships between the 2-D observations and 3-D co-ordinates of object points. By solving the collinearity equations the 3-D co-ordinates of these object points can be estimated. The three-dimensional right-handed Cartesian co-ordinate system is normally used as the object space co-ordinate system. The image co-ordinate system is also a three-dimensional right handed Cartesian co-ordinate system, with the *x* and *y* axes being in the image plane and *z* axis being toward the perspective centre of the camera. Figure 5 illustrates the object co-ordinate system *XYZ* and image co-ordinate system *xyz*.
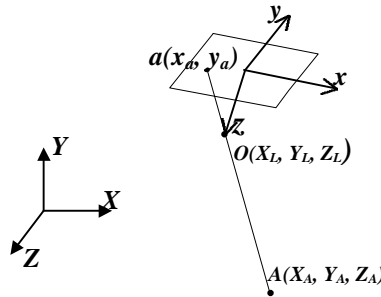

Figure 5 The object and image co-ordinate systems

The co-ordinates of the perspective centre $O(X_L, Y_L, Z_L)$ of the camera are related to object space co-ordinate system *XYZ* and the angular relationship between the image and the object co-ordinate systems can be described by a 3×3 orthogonal rotation matrix *M*. Nine elements are involved in the rotation matrix, but only three independent parameters are involved in the matrix *M*. They are **w**, **f** and **k**, the three sequential rotation angles around **X**, **Y** and **Z** axes respectively. If an object point $A(X_A, Y_A, Z_A)$ is imaged by a camera and located at point $a(x_a, y_a)$ on the image plane, a straight line can be projected from the point *A* through the perspective centre $O(X_L, Y_L, Z_L)$ of the camera onto the point *a* on the image plane. Ideally the line segments *AO* and *aO* should be on the same line, i.e., they are collinear and the collinearity equations are established as follows (Wolf, 1983)

$$x_a = -c\frac{m_{11}(X_A - X_L) + m_{12}(Y_A - Y_L) + m_{13}(Z_A - Z_L)}{m_{31}(X_A - X_L) + m_{32}(Y_A - Y_L) + m_{33}(Z_A - Z_L)}$$
$$y_a = -c\frac{m_{21}(X_A - X_L) + m_{22}(Y_A - Y_L) + m_{23}(Z_A - Z_L)}{m_{31}(X_A - X_L) + m_{32}(Y_A - Y_L) + m_{33}(Z_A - Z_L)}$$

(6)

where m_{11} - m_{33} are 9 elements of the rotation matrices *M* which describe the orientation of the cameras. These collinearity can be used in intersection (estimating the 3-D co-ordinates of the object points with known camera parameters), resection (estimating the camera parameters with known 3-D control points) and bundle adjustment (simultaneously estimating the 3-D co-ordinates of the object points and the camera parameters with all parameters treated as unknown parameters). When departures from the collinearity occur because of other media between the camera and the object it may become necessary to estimate further parameters to

model these departures. Another useful functional model is the DLT (Direct Linear Transformation) model. The DLT model proposed by Abdel-Aziz and Karara (1971) is an alternate formulation of the normal functional model. The DLT model is often used because it is quick to compute and also encompass some camera interior parameters such as the co-ordinates of the principal point (x_p, y_p) and the principal distances c_x and c_y.. Eleven DLT parameters are used which contain 10 camera physical parameters, of which six are exterior parameters $(X_L, Y_L, Z_L, \omega, \phi, \kappa)$ and four are interior parameters (x_p, y_p, c_x, c_y). With the lens distortions considered previously, the modified collinearity equations become

$$f_x = (x - \Delta x_p) + \Delta x_r + \Delta x_d + (c_0 + \Delta c)\frac{M_1}{M_3}, \qquad f_y = (y - \Delta y_p) + \Delta y_r + \Delta y_d + (c_0 + \Delta c)\frac{M_2}{M_3} \qquad (7)$$

Intersection is the procedure of determining the 3-D co-ordinates of the object points by intersecting lines projected from their corresponding points on the camera image planes (Wolf 1983; Karara 1989). In this process the camera parameters are required to be known. If an object point $A(X_A, Y_A, Z_A)$ is imaged by m cameras and located at the image points $a_1(x_1, y_1)$, $a_2(x_2, y_2)$, ..., $a_m(x_m, y_m)$ respectively, a straight line can be projected from each image point. Ideally these m lines should intersect at one point in the object space and that point should be $A(X_A, Y_A, Z_A)$. However, errors are inevitable during the measurement procedures. These lines will not intersect at the same point and the co-ordinates of the point are overdetermined. Using the least squares method (based on the collinearity equations) the 3D co-ordinates of the object point can be estimated. During the intersection process since the camera parameters are known, (X_{iL}, Y_{iL}, Z_{iL}) and $(m_{i11} ... m_{i33})$ are constants, where $i = 1, 2, ..., m$. The only unknown parameters in the collinearity equations are (X_A, Y_A, Z_A), the 3D co-ordinates of each object point. To solve for the three unknown parameters, this object point must appears on at least two images, which will give four equations and the least squares method can be applied for the best solution. There are two possible ways to solve for the three unknowns (X_A, Y_A, Z_A) in the collinearity equations. One is a direct solution which rearranges the collinearity equations into a linear form, the other is an iterative solution which keeps the collinearity equations in the original non-linear form. The latter solution is more rigorous because it minimises the sum of the squares of the residuals on the image planes. However starting values are required for the 3-D co-ordinates.

Resection is a procedure of determining camera exterior parameters $(X_L, Y_L, Z_L, \omega, \phi, \kappa)$ with known spatial control points (Thompson 1975; Slama 1980; Atkinson 1996). Space resection by DLT is one of the well known direct methods which transforms the collinearity equations into the linear form to avoid the requirement for the starting values. The standard DLT equations include 11 parameters which are related to the six camera exterior parameters $(X_L, Y_L, Z_L, \boldsymbol{w}, \boldsymbol{f}, \boldsymbol{k})$. The interior parameters can normally be ignored in the resection process. These equations can be solved directly by linear least squares estimation.

The bundle adjustment, developed by D.C. Brown in the 1960's (Brown 1976). It has also been widely used in the close range industrial photogrammetry (Granshaw 1980; Karara 1989; Fraser 1992; Atkinson 1996) and has been found to be a powerful tool in the high accuracy 3D measurement. Supposing m cameras are used to measure n object points. If all of these object points appear on all of the cameras, there will be $2mn$ equations in total and $(3n+6m)$ unknown parameters to be solved (provided that the camera interior parameters are fixed). The number of equations $2mn$ is usually much larger than the number of unknown

parameters ($3n+6m$). So these unknown parameters can be solved simultaneously. In general, the functional model in close range photogrammetry can be expressed as

$$f(x_1, x_2, x_2') = l \tag{8}$$

where $x_1 = (X, Y, Z)$ denotes a vector of the 3D co-ordinates of the object points, $x_2 = (X_L, Y_L, X_L, w, f, k)$ denotes a vector of the camera exterior parameters, $x_2' = (x_P, y_p, Dc, k_1, k_2, k_3, p_1, p_2)$ denotes a vector of the camera interior parameters and l represents the observed image co-ordinates. The linearized functional model may be written as

$$\begin{bmatrix} A_1 & A_2 \end{bmatrix} \begin{bmatrix} \Delta x_1 \\ \Delta x_2 \end{bmatrix} = b \tag{9}$$

in which $A_1 = \dfrac{\partial f}{\partial x_1}$ is a $2mn \times 3n$ matrix, and $A_2 = \dfrac{\partial f}{\partial x_2}$ is a $2mn \times 6m$ matrix. The unknown parameters can then be estimated by the simultaneous least squares estimation provided that the number of observations is equal to, or more than, that of the unknown parameters and the starting values of these parameters are known. The corrections to the parameters are estimated by

$$\Delta x = (A^t W_l A)^{-1} A^t W_l b = N^{-1} A^t W_l b \tag{10}$$

in which

$$N = \begin{bmatrix} A_1^t W_l A_1 & A_1^t W_l A_2 \\ A_2^t W_l A_1 & A_2^t W_l A_2 \end{bmatrix} = \begin{bmatrix} A_{11} & A_{12} \\ A_{21} & A_{22} \end{bmatrix} \tag{11}$$

6. EQUIPMENT

Retro-reflective materials are regularly used by photogrammetrists to obtain bright points sources of light which stand out from the background of a scene. These materials can, in theory, be up to 2000 times brighter than a perfectly diffuse white material. This can result in an image with only targeted features above the noise floor of the sensor. The benefits to photogrammetrists are: high image location accuracy and high signal to noise leading to easy of recognition and the use of a single threshold. To get the best results from such materials the light source must be within fractions of a degree from the target. Fortunately reasonable results can still be obtained with the light source at higher angles. Targets can be used for the purposes of determining camera orientation and stability; strips of the material might be used for lens calibration; or retro-reflective material could be used as a background light absorber allowing large amounts of light to be used without unduly lighting the background; or it may be possible to create retro-reflective particles. Two sources of errors are worth noting. The first error concerns the screen printed mask used by some to produce circular targets with a black background reported a -30μm to +30μm shift in the location of a retro-reflective target at angles of -40 and 40 degrees respectively. This error was found to be independent of target size or distance to the camera. Ahn & Kotowski (1997) have shown that if large targets are used then perspective distortion will also produce an error in target location. Both errors can be avoided by using small punched targets.

Lasers are often used to provide light sheets or target points. It should be noted that there are some draw-backs caused by the coherence of the laser light due to speckle. Speckle patterns are sometimes visible and the size varies with several parameters such as the aperture of the lens. However, it may not be possible for the image to reveal the speckle in the image if the speckle is much smaller than the pixel size but the image will be noisy as a result. Alternatively the speckle pattern may appear in the image in its characteristic granular form with an average speckle size bigger than the pixel spacing. A subtle effect is caused when the size of the illumination is small where it is not possible to form a speckle pattern but where the contributions across the image are nevertheless unevenly influenced by the interference. Under these conditions an apparently Gaussian shaped spot may be located inaccurately by a centroiding algorithm (Clarke & Katsimbrus, 1994).

7. CONCLUSION

The fundamentals of photogrammetric methods of extracting high precision information from CCD images have been presented. The material in this paper is not new but may be unfamiliar to researchers in this area. It is hoped that by pointing to a wealth of research results in the photogrammetric area a rich source of material might be opened up to others. By applying these methods and techniques to the measurement of heat and fluid flow it is expected that errors will be reduced and the imaging process will be better understood.

8. REFERENCES

Abdel-Aziz, Y. & Karara, H.M. 1971. Direct Linear Transformation From Comparator Co-ordinates into Object Space Co-ordinates in Close Range Photogrammetry. Papers from the American Society of Photogrammetry Symposium on Close Range Photogrammetry, Urbana, Illinois. 433, pp. 1-18.

Ackerman, F.,1984. Digital image correlation: performance and potential application in photogrammetry, Photogrammetric Record, 11(64), pp. 429-439.

Atkinson, K.B. (Ed), 1996. Close Range Photogrammetry and Machine Vision. Whittles Publishing, UK. 371 pages.

Ahn, S.J. & Kotowski, R. 1997. Geometric image measurement errors of circular object targets. Optical 3D Measurement Techniques IV.

Beyer, H.A., 1990. Linejitter and Geometric calibration of CCD cameras. Photogrammetric Engineering & Remote Sensing, Vol 45. pp. 17-32.

Brown, D.C. 1976. The Bundle Method -- Progress and Prospects. International Archives of Photogrammetry, 21(3) Paper 303: 33 pages

Chen, J. Clarke, T.A. & Robson. S., 1993. An alternative to the epipolar method for automatic target matching in multiple images for 3-D measurement. Optical 3-D measurements techniques II, Pub. Wichmann, Karlsruhe: 197-204.

Chen, J. Clarke, T.A. Cooper, M.A.R. Grattan, K.T.V.G. 1994., An optimised target matching based on a 3-D space intersection and a constrained search for multiple camera views, Videometrics III. SPIE Vol. 2350. Boston. pp. 324 - 335.

Chen, J. Robson, S. Cooper, M.A.R. & Taylor, R.N., 1996. An evaluation of three different image capture methods for measurement and analysis of deformation within a geotechnical centrifuge. International Archives of Photogrammetry and Remote Sensing. Vol. XXXI, Part B5, pp. 70-75.

Clarke, T.A. Cooper, M.A.R. & Fryer, J.G., 1993. An estimator for the random error in subpixel target location and its use in the bundle adjustment. Optical 3-D measurements techniques II, Pub. Wichmann, Karlsruhe:161-168.

Clarke, T.A. 1994, An analysis of the properties of targets uses in digital close range photogrammetric measurement, Videometrics III. SPIE Vol. 2350. Boston. pp. 251- 262.

Clarke, T.A. & Katsimbris, A. 1994. The use of diode laser collimators for targeting 3-D objects, International Archives of Photogrammetry and Remote Sensing, XXX(5): 47-54.

Clarke, T.A. 1995., A frame-grabber related error in subpixel target location. Photogrammetric Record. Vol XV. No 86. pp. 315-322.

Dhond, U.R. & Aggarwal, J.K. 1991. A cost-benefit analysis of a third camera for stereo correspondence. Int. Journal of Computer Vision. 6:1, pp. 39-58.

Forlani, G. Giussani, A. Scaioni, M. and Vassena, G. 1996. Target detection and epipolar geometry for image orientation in close-range photogrammetry. ISPRS Vol XXXI, Part B5. pp. 518-523.

Fraser, C.S. 1992. Photogrammetric Measurement to One Part in a Million. Photogrammetric Engineering & Remote Sensing, Vol 58. No 3. pp. 305-310.

Granshaw, S.I. 1980. Bundle Adjustment Methods in Engineering Photogrammetry. Photogrammetric Record, Vol. 10, No. 56, pp. 181-207.

Gruen, A. & Baltsavias, E.P., 1987. Geometrically constrained multiphoto matching. Intercommission conference on fast processing of photogrammetric data, Interlaken, Switzerland. pp. 204-230.

Hahn, M., 1993. Measurement by image matching - state of the art in digital photogrammetry. Photogrammetric Week 93, Pub. Wichmann, Karlsruhe, Ed. D. Fritsch, & D. Hobbie, 318 pages.

Haralick, R.M, and Shapiro, L.G. 1993. Computer and Robot Vision Volume II. Published by Addison-Wesley Publishing Company Inc. USA. 630 pages.

Höflinger, W. & Beyer, H.A., 1993. Evaluation and the Geometric Performance of a Standard S-VHS Camcorder. SPIE Vol. 2067. Videometrics. pp. 104 - 114.

Karara, H.M.1989. Non-topographic Photogrammetry. American Society for Photogrammetry and Remote Sensing. Falls Church, Virginia, 445 pages.

Maas, 1995. Determination of velocity fields in flow topography sequences by 3-D least squares matching. Optical 3-D measurements techniques II, Pub. Wichmann, Karlsruhe: pp. 366-376.

Marten, W. Mauelshagen, L. & Pallaske., 1994. Digital orthoimage-system for architectural representation. ISPRS Journal of Photogrammetry and Remote Sensing. 49(5): pp. 16-22.

Mikhail, E.M. Akey, M.L. & Mitchel, O.R. 1984. Detection and sub-pixel location of photogrammetric targets in digital images. Photogrammetria. Vol 39. pp. 63-93.

Mitchell, H.L. and Pilgrim, L.J., 1987. Selection of an image matching algorithm. Symposium on the applicaiton of Close Range Photogrammetry, Melbourne, Australia.

Robson, S. Clarke, T.A. & Chen, J., 1993. The suitability of the Pulnix TM6CN CCD camera for photogrammetric measurement. SPIE Vol. 2067, Videometrics II, pp 66-77.

Rosenholm, D., 1987. Least Squares Matching method: some experimental results. Photogrammetric Record. 12(70). pp 493-512.

Sabel, J.C. van Veenendaal, H.L.J. and Furnee, 1993. PRIMAS, a real time 3D motion analysis system. Optical 3-D Measurement Techniques II. Published by Wichmann, Karlsruhe, pp. 530-537.

Seitz, P. Vietze, O. & Spirig, T. 1995. From pixels to answers - recent developments and trends in electronic imaging. ISPRS. Vol 30. Part 5W1. pp. 2-12.

Shortis, M.R. Clarke, T.A., Short, T. 1994., A comparison of some techniques for the subpixel location of discrete target images, Videometrics III. SPIE Vol. 2350. Boston. pp. 239-250.

Shortis, M.R. Snow, W.L and Goad, W.K., 1995. Comparative geometric tests of industrial and scientific CCD cameras using plumb line and test range calibrations. *International Archives of Photogrammetry and Remote Sensing*, 30(5W1): 53-59.

Slama, C.C. (Ed), 1980. Manual of Photogrammetry. (Fourth Edition). American Society for Photogrammetry, Falls Church, Virginia, 1056 pages.

Thompson, E.H. 1975. Resection in Space. Photogrammetric Record, 8(45): April 1975, pp. 333-334.

Wang, X. & Clarke, T.A. 1996. An algorithm for real-time 3-D measurement. ISPRS Vol 31. Part B5. pp. 587-592.

Wolf, P.R. 1983. Elements of Photogrammetry. McGraw-Hill Inc., New York, 628 pages.

PAPER REFERENCE

Clarke, T.A. & Wang, X. 1998. Extracting high precision information from CCD images. Proc. ImechE Conf., Optical methods and data processing for heat and fluid flow. City University, pp. 311-320.